Temperature-Induced Single-Crystal-to-Single-Crystal Transformations and Structure-Directed Effects on Magnetic Properties

ARTICLE *in* INORGANIC CHEMISTRY · NOVEMBER 2007

Impact Factor: 4.76 · DOI: 10.1021/ic700867b · Source: PubMed

5 AUTHORS, INCLUDING:

Yves-Marie Legrand
Université de Montpellier
61 PUBLICATIONS **501** CITATIONS
SEE PROFILE

Pierre Rabu
University of Strasbourg
148 PUBLICATIONS **3,079** CITATIONS
SEE PROFILE

Inorg. Chem. **2007**, *46*, 9083–9089

Temperature Induced Single-Crystal-to-Single-Crystal Transformations and Structure Directed Effects on Magnetic Properties

Yves-Marie Legrand,[†] Arie van der Lee,[†] Nathalie Masquelez,[†] Pierre Rabu,*[,‡] and Mihail Barboiu*[,†]

Institut Européen des Membranes - UMR-CNRS 5635, Place Eugène Bataillon, CC 047, F-34095 Montpellier, Cedex 5, France, and Institut de Physique et Chimie des Matériaux de Strasbourg, UMR 7604 CNRS - Université Louis Pasteur, Groupe des Matériaux Inorganiques, 23, rue du Loess, F-67034 Strasbourg, France

Received May 5, 2007

The binding of Co^{II}, Ni^{II}, and Cu^{II} cations to the lithium 3-pyridinesulfonate ligand in an aqueous solution leads to single crystals of coordination polymers **1**–**3**. The solid-state architectures of **1**–**3** which resulted from the combination of ligand-water heterocomplexation processes are linear coordination polymers packed into parallel alternatively stratified layers. These layers are interconnected through intermolecular hydrogen-bonding interactions occurring between the coordinated water molecules and the noncoordinating oxygen atoms of the sulfonate groups. Consequently, this leads to the formation of the cross-linked 3D (**1**, **2**) or layered 2D (**3**) networks exhibiting 12-point or four-point hydrogen bond contacts between each unit with eight or four adjacent neighbors, respectively. The reversible structural rearrangement of these frameworks proceeds from the "relaxed" room-temperature phase to the "contracted" low-temperature phase in response to an external thermal stimulus. The reversibility of the contraction/relaxation process has been tested and confirmed by X-ray analysis. Motions toward shortening intermolecular distances have the consequence of increasing the degree of magnetic interaction between the metal ions. The magnetic measurements carried out in the range 1.8–400 K on the three compounds show an unusual change from antiferromagnetic to ferromagnetic behavior related to the structural variations recorded at low temperatures and to the loss of water above 350 K.

Introduction

Much effort has been devoted over the past decades to the design and the controlled crystallization of coordination networks based on transition-metal ions and multifunctional bridging ligands owing to their potential applications such as magnetism, electric conductivity, molecular absorption, and heterogeneous catalysis. Metal-organic open frameworks (MOFs),[1] 3D lamellar or tubular crystalline coordination polymers,[2] and metal- or cluster-mesogenic structures[3] have been used as scaffolds for designing materials with unique electronic and magnetic properties. Designing supramolecular crystalline devices with molecules that encode well-defined noncovalent motifs has recently attracted intense interest not only for their potential applications as new functional materials but also for their fascinating structural and super-

* To whom correspondence should be addressed. E-mail: mihai.barboiu@iemm.univ-montp2.fr (M.B.), Pierre.rabu@ipcms.u-strasbg.fr (P.R.).

[†] Institut Européen des Membranes - UMR-CNRS 5635.

[‡] Université Louis Pasteur.

(1) (a) Férey, G.; Mellot-Draznieks, C.; Serre, C.; Millange, F. *Acc. Chem. Res.* **2005**, *38*, 217−225. (b) Kitagawa, S.; Kitaura, R.; Noro, S. I. *Angew. Chem., Int. Ed.* **2004**, *43*, 2334−2375. (c) Rao, C. N. R.; Natarajan, S.; Vaidhyanathan, R. *Angew. Chem., Int. Ed.* **2004**, *43*, 1466−1496. (d) Batten, S. R. *Curr. Opin. Solid State Mater. Sci.* **2001**, *5*, 107−114.

(2) (a) Yamada, K.; Yagishita, S.; Tanaka, H.; Tahoyama, K.; Adachi, K.; Kaizaki, S.; Kumagai, H.; Inoue, K.; Kitaura, R.; Chang, H. C.; Kitagava, S.; Kawata, S. *Chem.--Eur. J.* **2004**, *10*, 2647−2660. (b) May, L. J.; Shimizu, G. K. H. *Chem. Commun.* **2005**, 1270−1272. (c) Tian, G.; Zu, G.; Yang, X.; Fang, Q.; Xue, M.; Sun, J.; Wei, Y.; Qiu, S. *Chem. Commun.* **2005**, 1396−1398. (d) Galan-Mascaros, J. R.; Dumbar, K. R. *Angew. Chem., Int. Ed.* **2003**, *42*, 2289−2293. (e) Luo, J.; Hong, M.; Wang, R.; Cao, R.; Han, L.; Yuan, D.; Lin, Z.; Zhou, Y. *Inorg. Chem.* **2003**, *42*, 4486−4488. (f) *J. Chem. Soc., Dalton Trans.* **2000**, *21*, special issue on crystal engineering.

(3) (a) Park, S. H.; Lee, C. E. *Chem. Commun.* **2003**, 1838−1839. (b) Kuriova, K.; Shibata, T.; Takada, A.; Nemoto, N.; Kimizuka, N. *J. Am. Chem. Soc.* **2004**, *126*, 2016−2021. (c) Camerel, F.; Antonetti, M.; Faul, C. F. J. *Chem.--Eur. J.* **2003**, *9*, 2160−2166. (d) Camerel, F.; Strauch, P.; Antonetti, M.; Faul, C. F. J. *Chem.--Eur. J.* **2003**, *9*, 3764−3771.

10.1021/ic700867b CCC: $37.00
Published on Web 09/29/2007

Scheme 1. Structure of Co^{II}, **1**; Ni^{II}, **2**; and Cu^{II}, **3** Complexes of Lithium 3-Pyridinesulfonate, **4**

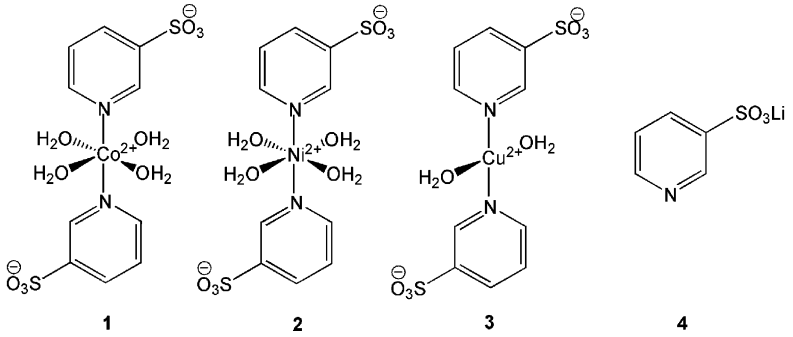

structural diversity.[4] The way from molecular to large crystalline systems depends both on the nature of its constituents and on the interactions between them. [5] Metal-directed self-assembly,[5] combined metal coordination, hydrogen-bonding (anion-templating),[6] and $\pi-\pi$ stacking[7] interactions have been extensively used as powerful tools for the spontaneous generation of such crystalline coordination superstructures. At this end, a given crystalline device may generate dynamic architectures depending on internal parameters (such as the nature of the binding subunits, the coordination geometry of the used metal ion, the metal ion/ligand ratio) or on external factors (such as the nature of the medium, the presence of specific molecules or anions, temperature, etc). Recent progress in this area has generated examples of dynamic multifunctional materials undergoing structural solid-state transitions upon constitutional rearrangements of their components (coordination geometry, nature of anions, etc.),[8] upon removal/reabsorption of guest, solvent, or ligand molecules,[9] and upon temperature induced transformations.[10] In this contribution we report on a contraction/relaxation process in the metal-sulfonatopyridine frameworks correlated with important changes in magnetic properties that occur at surprisingly low temperatures. This phenomenon seems here to be governed by small variation of the hydrogen bonding between water molecules and sulfonate groups. Such dynamic structural changes in metal coordination behavior can lead for example to their use in sensing adaptive devices. Herein we describe the chemistry along with the structure-magnetism relationship of [Co(3-pyridinesulfonate)$_2$(H_2O)$_4$] **1**, [Ni(3-pyridinesulfonate)$_2$-(H_2O)$_4$] **2**, and [Cu(3-pyridinesulfonate)$_2$(H_2O)$_2$] **3** complexes (Scheme 1).

Results and Discussions

Synthesis and Solid-State Structure of Compounds 1−3. Complexation of $CoCl_2$·$6H_2O$, $NiCl_2$·$6H_2O$, and $CuCl_2$·$2H_2O$ in an aqueous solution of lithium 3-pyridinesulfonate, **4**, produced at room temperature, almost quantitatively pink, light-green and light-blue, single crystals of coordination compounds **1**−**3**, respectively (Scheme 1). The unit cell of **1** was previously reported in the literature, but structure data are limited to indexation data. The molecular and crystal packing structures of **1**−**3** are presented in Figure 1. Single-crystal analysis shows that the structure of complexes **1** and **2** are isostructural but different from **3**. In **1** and **2**, the Co^{II} and Ni^{II} ions are octahedrally coordinated by two anionic ligands **4** and four water molecules (Figure 1a). In structure **3**, the Cu^{II} ions are octahedrally coordinated by two ligands **4**, two water molecules, and two sulfonate moieties of two adjacent ligands **4** (Figure 1b). The average $Co^{II}-N_{Py}$, $Ni^{II}-N_{Py}$, and $Cu^{II}-N_{Py}$ distances are 2.15, 2.10, and 1.98 Å, respectively, and the average $M^{II}-OH_2$ distance is about 2.00 Å.

This results in the emergence of rigid preorganized linear building blocks. (Figure 1a,b). The noncoordinating oxygen atoms of sulfonate moieties form hydrogen bonds with the coordinated water molecules of the neighboring units (d_{O-O} = 2.80 Å for **1** and **2**; d_{O-O} = 2.68 Å for **3**). Two such independent H-bonding interactions between two units are

(4) (a) *Acc. Chem Res.* **2005**, *4*, special issue on molecular architectures. (b) Reddy, D. S.; Duncan, S.; Shimizu, G. K. H. *Angew. Chem., Int. Ed.* **2003**, *42*, 1360−1364. (c) Noveron, J. C.; Lah, M. S.; Del Sesto, R. E.; Arif, A. M.; Miler, J. S.; Stang, P. J. *J. Am. Chem. Soc.* **2002**, *124*, 6613−6625.

(5) For recent reviews on metal ion metal self-assembly, see for example: (a) Leininger, S.; Olenyuk, B.; Stang, P. J. *Chem. Rev.* **2000**, *100*, 853−908. (b) Swiegers, G. F.; Malfetese, T. F. *Chem. Rev.* **2000**, *100*, 3483−3538. (c) Holliday, B. J.; Mirkin, C. A. *Angew. Chem.* **2001**, *113*, 2076−2097; *Angew. Chem., Int. Ed.* **2001**, *40*, 2022−2043. (d) Seidel, S. R.; Stang, P. J. *Acc. Chem. Res.* **2002**, *35*, 972−983.

(6) (a) Schmuck, C. *Angew. Chem.* **2003**, *115*, 2552−2556; *Angew. Chem., Int. Ed.* **2003**, *42*, 2448−2451. (b) Oh, K.; Jeong, K.-S.; Moore, J. S. *Nature* **2001**, *414*, 889−893. (c) Janiak, C. *J. Chem. Soc., Dalton Trans.* **2000**, 3885−3896. (d) Khlobystov, N. A.; Blake, A.; Champness, N. R.; Lemenovskii, D. A.; Majouga, A. G.; Zyk, N. V.; Schroder, M. *Coord. Chem. Rev.* **2001**, *222*, 155−192, and references therein. (e) Turner, D. R.; Spencer, E. C.; Howard, J. A. K.; Tocher, D. A.; Steed, J. W. *Chem. Commun.* **2004**, 1352−1353. (f) Turner, D. R.; Smith, B.; Goeta, A. E.; Evans, I. R.; Tocher, D. A.; Howard, J. A. K.; Steed, J. W. *CrystEngComm* **2004**, *6*, 633−641. (g) Blondeau, P.; van der Lee, A.; Barboiu, M. *Inorg. Chem.* **2005**, *44*, 5649−5653. (h) Noveron, J. C.; Lah, M. S.; del Sesto, R. E.; Arif, A. M.; Miler, J. S.; Stang, P. J. *J. Am. Chem. Soc.* **2002**, *124*, 6613−6625. (i) Uemura, K.; Kitagawa, S.; Kondo, M.; Fukui, K.; Kitaura, R.; Chang, H. C.; Mizutani, T. *Chem.--Eur. J.* **2002**, *8*, 3587−3600. (j) Hassenknopf, B.; Lehn, J.-M.; Boumediene, N.; Dupont-Gervais, A.; Van Dorsselaer, A.; Kneisel, B.; Fenske, D. *J. Am. Chem. Soc.* **1997**, *119*, 10956−10962.

(7) (a) Barboiu, M.; Vaughan, G.; Kyritsakas, N.; Lehn, J. M. *Chem.--Eur. J.* **2003**, 9, 763−769. (b) Barboiu, M.; Vaughan, G.; Kyritsakas, N.; Lehn, J. M. *Proc. Natl. Acad. Sci. U.S.A.* **2002**, *99*, 5201−5206. (c) Dumitru, F.; Petit, E.; van der Lee, A.; Barboiu, M. *Eur. J. Inorg. Chem.* **2005**, *21*, 4255−4262. (d) Barboiu, M.; Petit, E.; Vaughan, G. *Chem.--Eur. J.* **2004**, *10*, 2263−2270.

(8) For recent papers on solid-state transformations based on the nature of coordination subunits, see for example: (a) Takaoka, K.; Kawano, M.; Tomiaga, M.; Fujita, M. *Angew. Chem., Int. Ed.* **2005**, *44*, 2151−2154. (b) Delgado, F. S.; Kerbellec, N.; Ruiz-Pérez, C.; Cano, J.; Lloret, F.; Julve, M. *Inorg. Chem.* **2004**, *45*, 1012−1020. (c) Simmons, C. J.; Stratmeier, H.; Hitchmann, M. A.; Riley M. *J. Inorg. Chem.* **2006**, *45*, 1021−1031. (d) Thompson, A. L.; Goeta, A. E.; Real, J. A.; Galet, A.; Carmen Munoz, M. *Chem. Commun.* **2004**, 1390−1391.

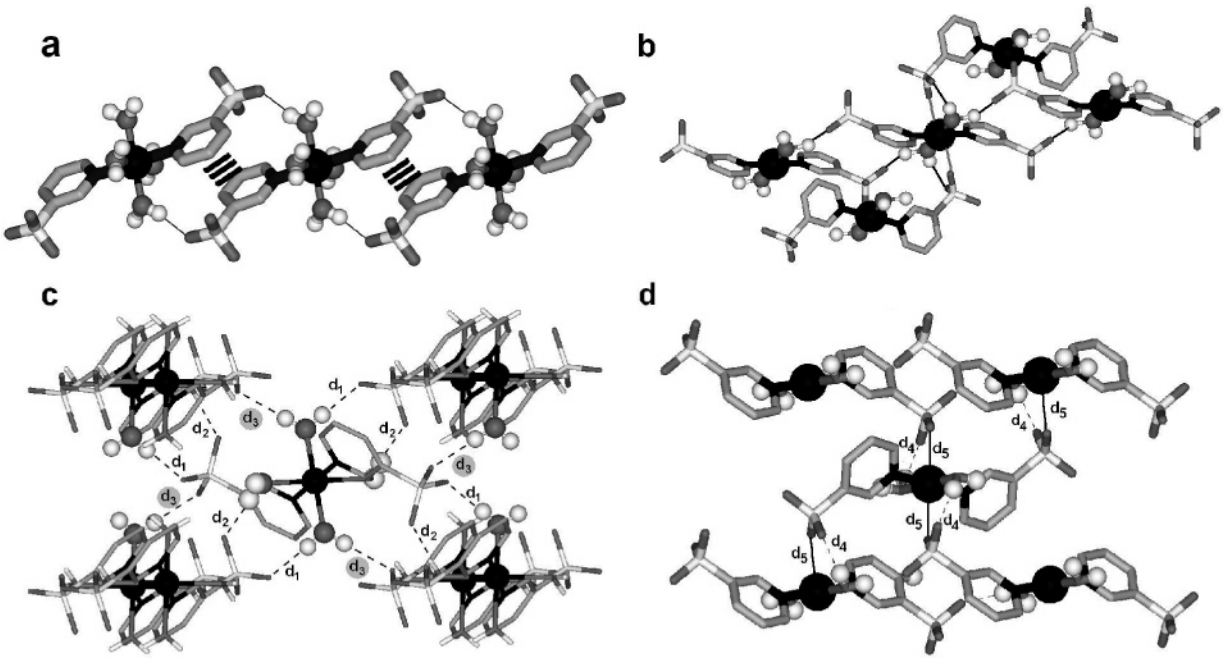

Figure 1. Crystal structures of **1**−**3**: side view in stick representation of (a) Co^{II} and Ni^{II} and (b) Cu^{II} linear coordination polymers. Stick representation of the crystal packing, resulting in the formation of the (c) cross-linked 3D (**1**, **2**) and (d) layered 2D (**3**) networks. The Co^{II}, Ni^{II}, and Cu^{II} ions are shown as black spheres; the water molecules are shown as a ball and stick representation.

complementarily assisted in structures **1** and **2** by favorable $\pi-\pi$ stacking interactions between neighboring terminal pyridine rings (centroïd−centroïd average distance of 3.66 (**1**) and 3.44 Å (**2**) corresponding to van der Waals contacts). The solid-state architectures of **1**−**3** which resulted from the combination of these heterocomplexation processes are linear coordination polymers, and in the crystal lattice they pack along the crystallographic *c*-axis, into parallel layers which are alternatively stratified. In the adjacent layers, the ligand planes on either side of the layer interface are rotated with respect to each other by 63° (**1**, **2**) (Figure 1a) and 73° (**3**) (Figure 1b). The two types of layers are connected through intermolecular hydrogen-bonding interactions occurring between H atoms of the coordinated water molecules and the noncoordinating oxygen atoms of the sulfonate groups (Figure 1c,d). Consequently, this leads to the formation of the cross-linked 3D (**1**, **2**) or of the layered 2D (**3**) networks exhibiting 12-point (Figure 1c) or four-point (Figure 1d) hydrogen bond contacts between each unit with eight or four adjacent neighbors, respectively. These patterns results in a regular disposition of the metal centers situated at the vertices of interpenetrating crystallographic cells (Figure 2c,d).

The 3D network of **1** (very similar to **2**) at 95 K results from the combination of three types of hydrogen bonds: one of these ($d_{3,O-O}$ = 2.88 Å, 95 K) is longer than the other ones ($d_{1,O-O}$ = 2.75 Å and $d_{2,O-O}$ = 2.71 Å, 95 K). Between 293 and 95 K, the 3D network of **1** is almost identical, apart from a major difference in the distance of the $d_{3,O-O}$ hydrogen bond. Indeed a difference of 0.13 Å is present ($d_{3,O-O}$ = 3.01 Å, 293 K) between the two temperatures. A survey of the Cambridge Structural Database (Figure 2Sb, Supporting Information) for hydrogen bonds between a sulfate and a water molecule (see Supporting Information) tends to indicate that above 3.0 Å the effect of hydrogen bonding is too weak to have an impact on the population of such bonds. Nonetheless, a close look at the crystal structure reveals that, even at 293 K ($d_{3,O-O}$ = 3.01 Å), the orientation of the hydrogen atom between the two heteroatoms is exactly the one expected for a hydrogen bond (O−H−O angle of 166°). Although we think it is reasonable to say that we observed a shortening of the $d_{3,O-O}$ bond, it is also fair to propose that, upon cooling, the d_3 hydrogen bond is formed, helped by favorable orientation of the packing at room temperature. The 2D network of **3** results from the combination of four hydrogen bonds ($d_{4,O-O}$ = 2.70 Å, 293 K) and four coordinative bonds ($d_{5,Cu-O}$ = 2.50 Å, 293 K) the Cu^{II} being linked on two sides by the neighboring sulfonate counterions.

Variable Temperature Single-Crystal Diffraction Experiments. Single-crystal diffraction data of **1**−**3** have been recorded at 293, 175, and 95 K. A remarkable contraction of the crystal cell of the Co^{II} complex **1** was observed with an important shortening of the d_3 H-bonds at low temperatures (Table 1, Figure 1S, Supporting Information).

(9) For recent papers on solid-state transformations based on guest, solvent, and water exchange, see for example: (a) Abe, T.; Shinozaki, K.; *Inorg. Chem.* **2005**, *44*, 849−851. (b) Rather, B.; Zaworotko, M. *J. Chem. Commun.* **2003**, 830−831. (c) Lu, Z.; Wang, X.; Liu, Z.; Liao, F.; Gao, S.; Xiong, R.; Ma, H.; Zhang, D.; Zhu, D. *Inorg. Chem.* **2006**, *45*, 999−1004. (d) Choi, H. J.; Suh, M. P. *J. Am. Chem. Soc.* **2004**, *126*, 15884−15851. ()e Lee, E. Y.; Suh, M. P. *Angew. Chem., Int. Ed.* **2004**, *43*, 2798−2801. (f) Matsuda, R.; Kitaura, R.; Kitagawa, S.; Kubota, Y.; Kobayashi, T. C.; Horike, S.; Takata, M. *J. Am. Chem. Soc.* **2004**, *126*, 14063−14070. (g) Wadas, T. J.; Wang, Q.-M.; Kim, Y.-J.; Flashenreim, C.; Blanton, T. N.; Eisenberg, R. *J. Am. Chem. Soc.* **2004**, *126*, 16841−16849. (h) Wu, C. D.; Lin, W. *Angew. Chem., Int. Ed.* **2005**, *44*, 1958−1961.

(10) For recent papers on solid-state transformations based on temperature variation, see for example: (a) Zhang, J. P.; Lin, Y. Y.; Zhang, W. X.; Chen, X. M. *J. Am. Chem. Soc.* **2005**, *127*, 14162−14163. (b) Hu, C.; Englert, U. *Angew. Chem., Int. Ed.* 2005, *44*, 2281−2283. Yuan, Z.; Lee, C. W.; Lee, S. H. *Angew. Chem., Int. Ed.* **2004**, *43*, 4197−4200. (c) Masaoka, S.; Tanaka, D.; Nakanishi, Y.; Kitagawa, S. *Angew. Chem., Int. Ed.* **2004**, *43*, 2530−2534.

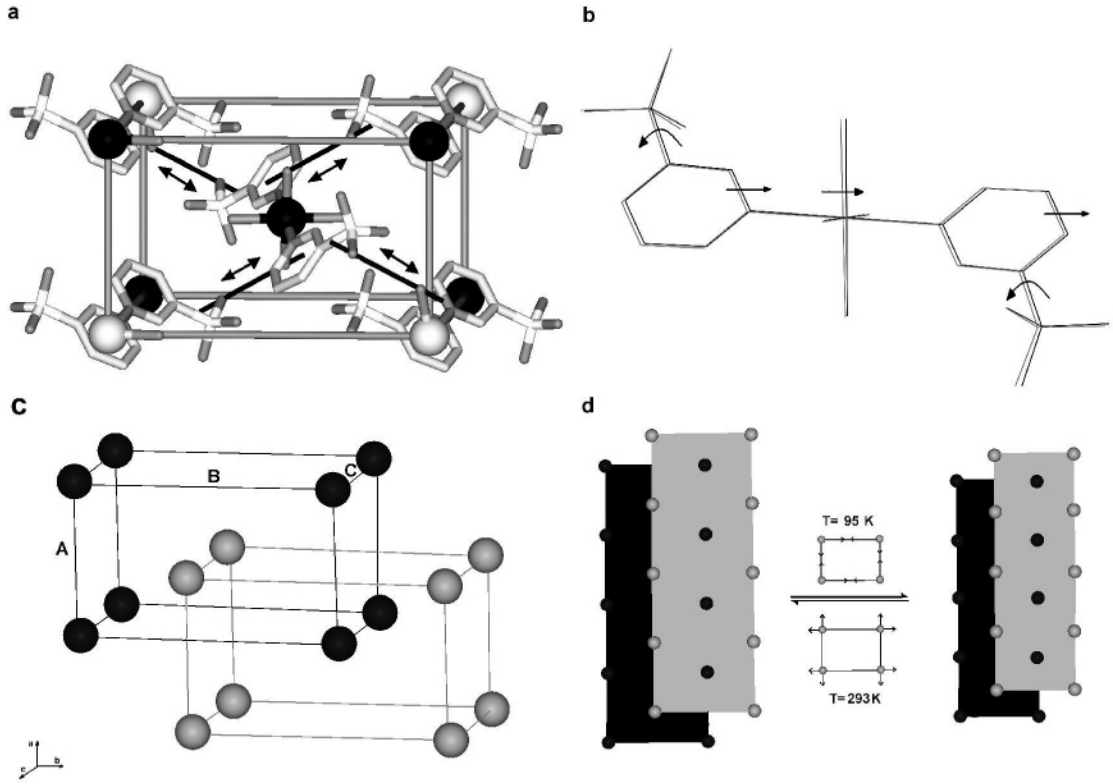

Figure 2. (a) 3D network of **1** with an important shortening of the d_3 H-bonds at low temperatures; (b) global translation along N−Co−N axis and subsequent rotation of sulfonate groups at low temperatures; (c) regular disposition of the metal centers situated at the vertices of interpenetrated crystallographic cells; and (d) reversible contraction/relaxation in the *b* and *c* axes with temperature.

Table 1. Selected d_3 H-Bond Lengths, the Cell Volume *V*, and the Distance between Co^{II} Centers Situated at the Vertices of Crystallographic Cells of **1** at 293, 175, and 95 K and Back to 293 K

T/K	d_3/Å	a_T/Å $\Delta a =$ $a_T - a_{293}$	b_T/Å $\Delta b =$ $b_T - b_{293}$	c_T/Å $\Delta c =$ $c_T - c_{293}$	V_T/Å^3 $\Delta a =$ $V_T - V_{293}$
293	3.012	7.581	12.663	8.720	830.0
		0.000	0.000	0.000	0.000
175	2.94	7.610	12.560	8.670	820.8
		+0.029	−0.103	−0.050	−9.2
95	2.89	7.628	12.504	8.631	815.1
		+0.047	−0.159	−0.089	−14.9
293	3.018	7.580	12.661	8.717	829.5
		−0.001	−0.002	−0.003	−0.5

Table 2. Selected d_3 H-Bond Lengths, the Cell Volume *V*, and the Distance between Ni^{II} Centers Situated at the Vertices of Crystallographic Cells of **2** and Cell Volume at 293, 175, and 95 K

T/K	d_3/Å	a_T/ÅΔ $a =$ $a_T - a_{293}$	b_T/ÅΔ $b =$ $b_T - b_{293}3$	c_T/Å $\Delta c =$ $c_T - c_{293}$	V_T/Å^3 $\Delta a =$ $V_T - V_{293}$
293	3.11	7.504	12.659	8.735	822.9
		0.000	0.000	0.000	0.000
175	3.06	7.483	12.617	8.711	814.9
		−0.021	−0.042	−0.024	−8.0
95	3.04	7.506	12.563	8.666	809.3
		+0.002	−0.096	−0.069	−13.6

Table 3. Selected d_4 H-Bond Lengths, d_5 Coordinative Bond Lengths, the Cell Volume *V*, and the Distance between Cu^{II} Centers Situated at the Vertices of Crystallographic Cells of **3** and Cell Volume at 293, 175, and 95 K

T/K	d_4/Å	d_5/Å	a_T/Å $\Delta a =$ $a_T - a_{293}$	b_T/Å $\Delta b =$ $b_T - b_{293}$	c_T/Å $\Delta c =$ $c_T - c_{293}$	V_T/Å^3 $\Delta a =$ $V_T - V_{293}$
293	2.68	2.47	9.044	9.009	9.552	704.9
			0.000	0.000	0.000	0.000
175	2.69	2.49	9.025	8.918	9.565	697.7
			−0.019	−0.091	+0.013	−7.2
95	2.71	2.50	9.004	8.858	9.576	692.6
			−0.040	−0.151	+0.024	−12.3

Four such contraction processes occur (Figure 2a), inducing a global translation of each molecular unit along the N−Co−N axis associated with a rotation of the sulfonate groups (Figure 2b). Our first interrogation was that, at room temperature, the change in bond length might arise from the disorder of the crystal structure, which was not the case as it can be seen in the single-crystal data. As a result, the Co^{II} ions are moving along the (*bc*) plane diagonal and contractions in the *b* and *c* axes were observed (Table 1, Figure 2, and Figure 1S, Supporting Information).

The same behavior was observed for the Ni^{II} complex **2**, but less important reductions in the *b* and *c* axes were observed (Table 2, Figure 1, Figure 2S, Supporting Information).

In the Cu^{II} complex **3**, within the 2D layers, an important reduction in the *b*-axis (Table 3, Figure 1d) was observed at low temperature. In the crystal lattice, the layers are alternatively stratified and pack upon the diagonal of the (*ac*) plane. Surprisingly, an initial contraction (293 K → 175 K) followed by a subsequent expansion (175 K → 95 K) of the d_4 H-bonds and d_5 coordinative bonds in the crystal were identified at low temperatures (Table 3, Figure 1, Figure 2S, Supporting Information). Such processes are well correlated with an initial shortening and subsequent lengthening of inter- and intraplanar distances of the layers at low temperature, corresponding to van der Waals contacts. As a result the Cu^{II}

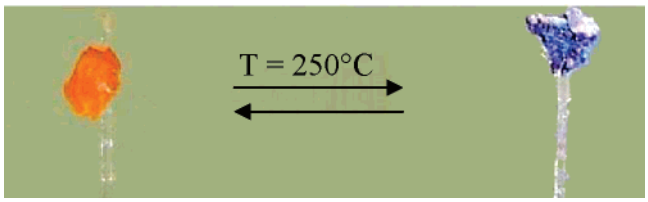

Figure 3. Pictorial representation of the dehydration and rehydration processes: the pink crystal of **1** turns blue upon dehydration and turns back to the original pink color upon rehydration.

ions running along the *b*-axis and important reduction in the *b*- and *c*-axes were observed (Table 3, Figure 2c,d).

The reversible structural rearrangement of the framework proceeds from the "relaxed" room-temperature to the "contracted" low-temperature phase in response to an external thermal stimulus. The reversibility of the contraction/relaxation process has been tested and confirmed by X-ray analysis.

Next, to investigate the removal of the coordinated water molecules, single crystals of **1** were heated progressively to 600 °C. DSC, TGA, and PXRD reveal that **1** could lose two water molecules at 125 °C and then two other water molecules at 225 °C (Figure 3S, Supporting Information). Upon heating, the initial pink crystal turned light blue and then blue (Figure 3). The coordinated water molecules have been eliminated in two distinct steps. The chromism of the crystal is principally ascribed to the well-known modification of the energy level of d orbitals of the Co^{II} induced by dehydration,[11b] just like for Co^{II} chloride in moisture indicating blue silica gel; this decreases the HOMO−LUMO energy gap in the complex which causes a blue shift of the absorption bands. The blue color of the dehydrated phase suggests a change of coordination mode, the environment becoming tetrahedral with the loss of two water molecules around the Co^{II} centers. Exposure to water vapors for several hours reverses the structural state, and the original material **1**, including the coordinated water molecule, is reconstituted. The PXRD patterns of dehydrated products were different from that of **1**. Very similarly, single crystals of **2** were analyzed following the above method; again DSC, TGA, and PXRD reveal that **2** could lose water molecules at slightly higher temperatures. The first two water molecules were released at 145 °C and the other two at 195 °C. Although in the case of **1** the TGA weight loss is sharp, this is not as abrupt for **2**. In both cases, **1** and **2** show a decomposition temperature around 450 °C. Finally, single crystals of **3** were heated progressively to 600 °C. Two water molecules were released at 198 °C, which correspond to the entire amount of water in the crystal, in opposition with the two previous cases, where only one-half of the coordinated water content is eliminated first, the other half being lost at higher temperatures.

(11) (a) Anagnostopoulos, A.; Matthews, R. W.; Walton, R. A. *Can. J. Chem.* **1972**, *50*, 1307−1314. (b) Ben-Salah, M.; Vilminot, S.; Richard-Plouet, M.; André, G.; Mhiri, T.; Kurmoo, M. *Chem. Commun.* **2004**, 2548−2549. (c) Chen, C. L.; Goforth, A. M.; Smith, M. D.; Su, C. Y.; Conrad zur Loye, H. *Angew. Chem., Int. Ed.* **2005**, *44*, 6673−6677.

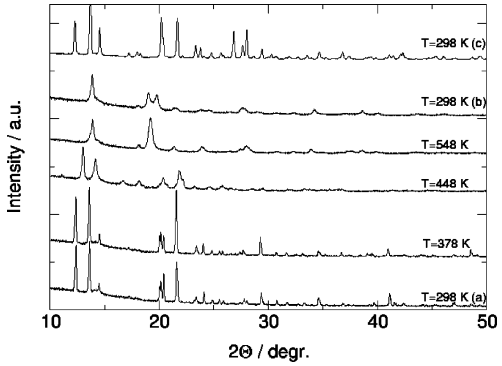

Figure 4. X-ray powder diffraction patterns for complex **1** at different temperatures: (a) a fresh sample complex, (b) the same sample after removal of four water molecules at 298 K, and (c) the same sample after exposure to a H_2O vapor.

The structural changes of the Co^{II} complex upon heating were followed by variable-temperature X-ray powder diffraction measurements. The structural quality of the starting powder was very good without any impurity phases present as is shown by full pattern matching calculations (see the Supporting Information). Figure 4 shows a first transition between 378 and 448 K corresponding to the first loss of two water molecules and a second transition between 448 and 548 K corresponding to the loss of the tighter bound water molecules. The first transition is accompanied by a loss in structural cohesion in view of the broadening of the diffraction peaks: typical full width at half maximum (fwhm) values near $2\Theta = 15°$ are 0.08° below and 0.24° above the first transition, respectively. The first fwhm is close to the instrumental resolution of the experimental setup, so that the broadening is solely due to a shortening of the domain length over which the X-rays scatter coherently. It is reasonable to postulate that this reduced coherence length is due to the loss of the two water molecules cross-linking the 3D network, whereas the second transition involves the two water molecules constituting the linear H-bond stacked ribbons. Both transitions are accompanied by a structural rearrangement, which however could not be quantified, because of the insufficient quality of the data. The same type of high variable-temperature experiments was performed using single crystals, but these data were not of sufficient quality to be analyzed in detail. The powder diffraction data collected at room-temperature right after cooling from the second transition point shows that the takeup of water has already begun, although it is certainly not finished. After an overnight exposure to a H_2O vapor the crystal structure is completely recovered as is shown by the upper diffractogram in Figure 4. The crystalline quality is even slightly improved compared to that of the initial powder, showing more peaks with higher intensities. The correspondence of the powder diffractogram with the single-crystal structure is shown in Figure 4S of the Supporting Information by an excellent Le Bail full pattern fit of a high quality powder of **1**. Subsequent Rietveld refinement showed that the structure can be refined to atomic resolution using these powder data.

Temperature-Dependent Magnetic Behavior. The three compounds **1**−**3** exhibit an original magnetic behavior related

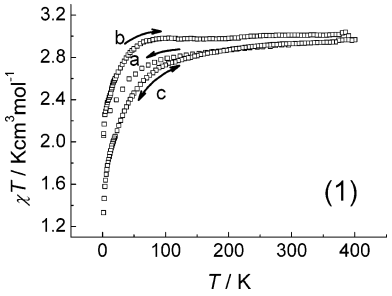

Figure 5. Temperature variation of the magnetic susceptibility as the χT product for complex **1**: (a) the initial cooling, (b) the heating back to high temperatures, and (c) the same sample after removal of two water molecules at 400 K (arrows indicate the variation in temperature).

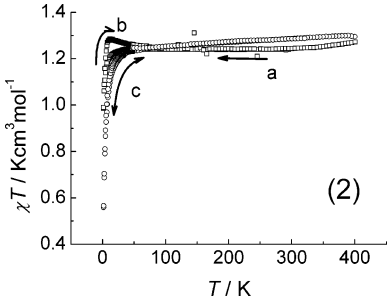

Figure 6. Temperature variation of the magnetic susceptibility as the χT product for complex **2**: (a) the initial cooling, (b) the heating back to high temperatures (squares), and (c) the same sample after removal of two water molecules at 400 K (circles). Arrows indicate the variation in temperature.

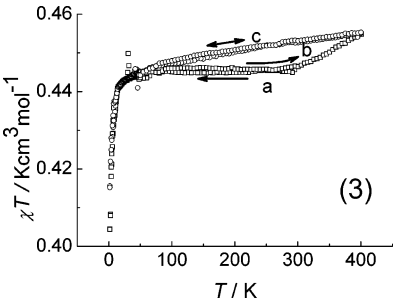

Figure 7. Temperature variation of the magnetic susceptibility as the χT product for complex **3**: (a) the initial cooling, (b) the heating back to high temperatures, and (c) the same sample after heating at 400 K. Arrows indicate the variation in temperature.

to the temperature-dependent structural features. The same behavior was observed on two different samples in each case.

The thermal variation of the magnetic susceptibility of the cobalt compound **1** $(C_3H_4NSO_3)_2Co{\cdot}4H_2O$ is presented in Figure 5. During the initial cooling of the sample (curve a), the magnetic susceptibility shows the typical behavior for quasi isolated octahedral high spin Co^{II} ions with a Curie constant $C = 2.99$ K·cm^3·mol^{-1} and the Weiss temperature $\theta = -0.92$ K, deduced from fitting the inverse susceptibility to the Curie−Weiss law above 150 K (not shown). The decrease of χT from 2.9 K·cm^3·mol^{-1} at 295 to 2.05 K·cm^3·mol^{-1} at 1.8 K, denoted by the negative value of the Weiss temperature, is likely related to the effect of spin−orbit coupling stabilizing an effective spin doublet state,[12,13] although the contribution of weak antiferromagnetic interactions could not be ruled out.

The remarkable event is the occurrence of a hysteretic behavior during the subsequent increase in temperature (curve b), with a significantly higher value of χT compared to the initial cooling, the two curves joining only at high temperature. Such difference can be ascribed either to a strong change of the spin−orbit coupling parameters, meaning a variation of the ligand field induced by low temperature, or even to a weak ferromagnetic coupling, the effect of which (increase of $\chi T(T)$) would compete with that of the spin−orbit coupling (decrease of $\chi T(T)$ with temperature). When heated at 400 K, compound **1** loses two water molecules. The magnetic moment is slightly lowered to the initial value. Decreasing the temperature, the dehydrated product **1′** exhibits again a regular decrease of the χT product but steeper than observed for the initial compound **1**. Moreover, the small value of 1.3 K·cm^3·mol^{-1} measured at 1.8 K compared to that usually expected for isolated Co^{II} suggests the existence of an antiferromagnetic coupling between the magnetic centers. Finally, the magnetization cycle at 1.8 K shown in the Supporting Information (Figure 5S) points out the absence of long-range magnetic ordering at the end of the thermal sequence and M(H) saturates at 2 μ_B, which is in the range observed for $S = {}^3/_2Co^{II}$. [12] It is worth noticing also that a subsequent reheating of the partially dehydrated product **1′** indicates a reversible variation of the magnetic susceptibility, in that case.

The magnetic findings for the nickel analogue **2** are qualitatively very similar to the precedent one as shown in Figure 6. In the initial cooling (a), the χT product shows a constant value of ca. 1.24 K·cm^3·mol^{-1} corresponding well to the expected behavior of isolated Ni^{II} ions in octahedral environment.[12,13] Accordingly, the fit of the inverse susceptibility to the Curie−Weiss law leads to $C = 1.25$ K·cm^3·mol^{-1} and $\theta = -0.22$ K. A slight decrease of the moment is observed below 50 K which can be due to a weak antiferromagnetic coupling and also to a zero-field splitting effect for the d^8 Ni^{II} ions. Amazingly, the $\chi T(T)$ curve exhibits a maximum of 1.284 K·cm^3·mol^{-1} at 14.85 K when reheating the sample (Figure 6b). This feature indicates thus a change of the couplings mediated through the H-bond network between the magnetic entities leading to an overall ferromagnetic behavior. The values overlay the initial curve only above 90 K. After partial dehydration at 400 K a slight increase of χT (1.29 K·cm^3·mol^{-1} at 400 K) is observed, and the product **2′** shows a regular decrease of the moment associated with weak antiferromagnetic interactions. This behavior is then reversible in temperature, and the magnetization versus field loop recorded at 1.8 K indicates no long-range ordering and typical value of saturation moment Ms ≈ 2.0 μ_B at 5 T for $S = 1$ Ni^{II} ions.

As shown in Figure 7, the copper compound **3** has a different behavior than **1** and **2**. Indeed, when cooling the compound (curve a), the moment is constant down to ca. 75 K with $\chi T = 0.44$ K·cm^3·mol^{-1}, and the Curie constant, $C = 0.446$ K·cm^3·mol^{-1}, agrees well to that expected for $S = 1/2$ Cu^{II} ions with $g = 2.18$.[12,13] The small decrease observed below 75 K is the signature of very weak antiferromagnetic

(12) Carlin, R. L. *Magneto-Chemistry*; Springer-Verlag: Berlin, 1986.
(13) Kahn, O. *Molecular Magnetism*; VCH: Weinheim, 1993.

interactions. In contrast with the two other compounds, **3** did not show a hysteresis when reheating the sample (Figure 7b). The same behavior was observed up to room temperature. Then χT increased gently up to 0.445 K·cm^3·mol^{-1} at 400 K. Decreasing the temperature down to 75 K, the curve (c) remains above the precedent, and the constant decrease is characteristic of an antiferromagnetic behavior. It is reversible, and no magnetic order was observed at 1.8 K. Thus heating at 400 K, which is well below that found for the total dehydration of **3**, should induce a structural variation responsible for the change in the coupling between the copper centers that are known to be particularly sensitive to small variations of the geometry of the exchange pathways.[14]

Conclusion

We have synthesized and characterized structurally and magnetically a new series of transition-metal molecular compounds resulting from the combination of 3-pyridinesulfonate-water heterocomplexation processes. The structures consist of cross-linked 3D (**1**, **2**) or layered 2D (**3**) networks exhibiting 12-point or four-point hydrogen bond intermolecular contacts with eight or four adjacent units, respectively. A reversible structural rearrangement of these frameworks was observed from a "relaxed" room-temperature phase to a "contracted" low-temperature (95 K) phase. Motions toward shortening intermolecular distances have a significant and rather unusual consequence on the magnetic interaction between the metal ions.

The structural results suggest that there could be a kind of competition between the ligand hindrance and hydrogen bonding for stabilizing the packing. At room temperature, in **1** and **2**, the H-bonds are dissimilar with one long O−O distance d_3. At low temperature the H-bond distances tend to be homogenized in the range of their usual value thanks to significant distortions. These distortions modify the overlap between magnetic orbitals and influence the spin polarization mechanism along the H-bonds resulting in different intermolecular magnetic interactions. Actually, coupling mediated through hydrogen bonding has been identified in many radical-based and transition-metal-based molecular magnets.[15,16] In the present case, the molecular magnetic centers (Co^{II}, Ni^{II}) are linked via three H-bonds d_1, d_2, and d_3 corresponding to as much interaction pathways. Hence the effective intermolecular interaction results from three competing interactions, and thermally induced distortions can modify the relative strengths of these interactions. As a result, a change from an antiferromagnetic to a ferromagnetic behavior is observed when cooling down to 1.8 K. Such variation is reminiscent to what was observed in several organic radical magnets in which the intermolecular coupling could be tuned either by the packing or by external pressure.[17,18] In some manner, in the present case, the thermal contraction seems to be as efficient as external pressure. It is worth noticing also that such a possibility of tuning the metal-to-metal interaction through H-bonds was recently suggested in a copper-palladium molecular compound.[16b]

The hysteresis of the magnetic susceptibility observed at low temperature in **1** and **2** is merely related to the structure of the water molecule network and to the modification of H-bonds accompanied by the distortions highlighted by the low-temperature structural analysis. The hysteretic magnetic behavior reveals that the low-temperature H-bond driven arrangement is stable enough to remain up to quite high temperatures. The same effect is not observed in **3**, which has a different structure involving only two water molecules around the copper centers, instead of four in **1** and **2**, and different coordination. Nevertheless an irreversible structural variation is suggested to occur above room temperature. The magnetic behavior was observed when cooling and reheating in a temperature range wider than for the structural investigation. Thus a temperature resolved structural study in the full range 1.8−400 K (and higher for complete in-situ dehydration) would be very interesting for accurate correlations with the magnetic behaviors. Such experiments are in progress.

Acknowledgment. This work, conducted as part of the award "Dynamic adaptive materials for separation and sensing Microsystems" (M.B.) made under the European Heads of Research Councils and European Science Foundation EURYI (European Young Investigator) Awards scheme in 2004, was supported by funds from the Participating Organizations of EURYI and the EC Sixth Framework Program. See www.esf.org/euryi. This research was supported in part by the CNRS, University of Montpellier 2 and Université Louis Pasteur, Strasbourg, France.

Supporting Information Available: Summary of the crystallographic data for compounds **1** and **2** (Table 1S), cell lengths vs temperature of **1**−**3** (Figure 1S), cell volume vs temperature of **1**−**3** (Figure 2Sa), Cambridge Structural Database survey of a hydrogen bond between a sulfate and a water molecule (Figure 2Sb), TGA analysis for **1**−**3** (Figure 3S), full pattern matching of **1** (Figure 4S), magnetization vs field curves of **1** and **2** (Figure 5S), and cif files. This material is available free of charge via the Internet at http://pubs.acs.org.

IC700867B

(14) Crawford, V. H.; Richardson, H. W.; Wasson, J. R.; Hodgson, D. J. *Inorg. Chem.* **1976**, *15*, 2107−2110.

(15) (a) Maruta, G.; Takeda, S.; Imachi, R.; Ishida, T.; Togami, T.; Yamaguchi, K. *J. Am. Chem. Soc.* **1999**, *121*, 424. (b) Ishida, T.; Tomioka, K.; Nogami, T.; Yoshikawa, H.; Yasui, M.; Iwasaki, F. *Chem. Phys. Lett.* **1995**, *247*, 7. (c) Daigoku, K.; Okada, A.; Nakada, K. *Chem. Phys. Lett.* **2006**, *430*, (4−6), 221. (c) Rajadurai, C.; Enkelmann, V.; Zoppellaro, G.; Baumgarten, M. *J. Phys. Chem. B.* **2007**, *111*, (17), 4327−4334, and references therein.

(16) (a) Valigura, D.; Moncol, J.; Korabik, M.; Púceková, Z.; Lis, T.; Mrozinski, J.; Melník, M. *Eur. J. Inorg. Chem.* **2006**, *22*, (19), 3813−3817. (b) Hanko, J.; Orendac, M.; Kuchar, J.; Zak, Z.; Cernak, J.; Orendacova, A.; Feher, A. *Solid State Comm.* **2007**, *142*, (3), 128.

(17) Sorai, M.; Nakano, M.; Miyazaki, Y. *Chem. Rev.* **2006**, *106*, 976−1031, and references therein.

(18) (a) Takahashi, M.; Turek, P.; Nakazawa, Y.; Tamura, M.; Nozawa, K.; Shiomi, D.; Ishikawa, M.; Kinoshita, M. *Phys. Rev. Lett.* **1991**, *67*, 746−748. (b) Takeda, K.; Mito, M.; Kawae, T.; Takumi, M.; Nagata, K.; Tamura, M.; Kinoshita, M. *J. Phys. Chem. B* **1998**, *102*, 671−676. (c) Matsushita, M. M.; Izuoka, A.; Sugawara, T.; Kobayashi, T.; Wada, N.; Takeda, N.; Ishikawa, M. *J. Am. Chem. Soc.* **1997**, *119*, 4369−4379.